Supporting Information -

Rapid crystallization and kinetic freezing of site-disorder in the lithium superionic argyrodite Li_6PS_5Br

Ajay Gautam[a,b], Marcel Sadowski[c], Nils Prinz[d], Henrik Eickhoff[e], Nicolò Minafra[a,b], Michael Ghidiu[a,b], Sean P. Culver[a,b], Karsten Albe[c], Thomas F. Fässler[e], Mirijam Zobel[d], Wolfgang G. Zeier*[a,b]

[a]*Institute of Physical Chemistry, Justus-Liebig-University Giessen, Heinrich-Buff-Ring 17, D-35392 Giessen, Germany.*

[b]*Center for Materials Research (LaMa), Justus-Liebig-University Giessen, Heinrich-Buff-Ring 16, D-35392 Giessen, Germany.*

[c]*Department of Materials Science, Technische Universität Darmstadt, Otto-Berndt-Straße 3, D-64287 Darmstadt, Germany.*

[d] *Department of Chemistry, University of Bayreuth, Universitätsstr.30, D-95440 Bayreuth, Germany.*

[e]*Department of Chemistry, Technische Universität München, Lichtenbergstrasse 4, D-85747 Garching bei München, Germany.*

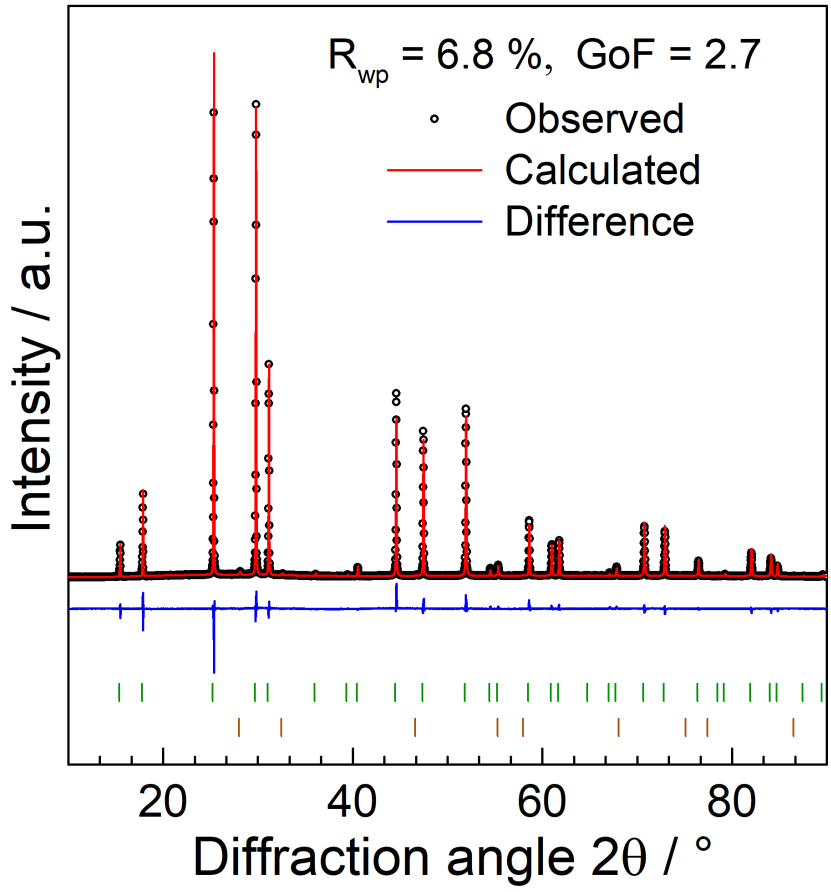

Figure S1: X-ray powder diffraction data for Li_6PS_5Br after 5 min heating followed by quenching and corresponding Rietveld refinement. Experimental data are shown in black and the red line denotes the calculated pattern, while the difference profile is shown in blue. Calculated positions of the Li_6PS_5Br and LiBr Bragg reflections are shown as green and dark orange vertical ticks, respectively.

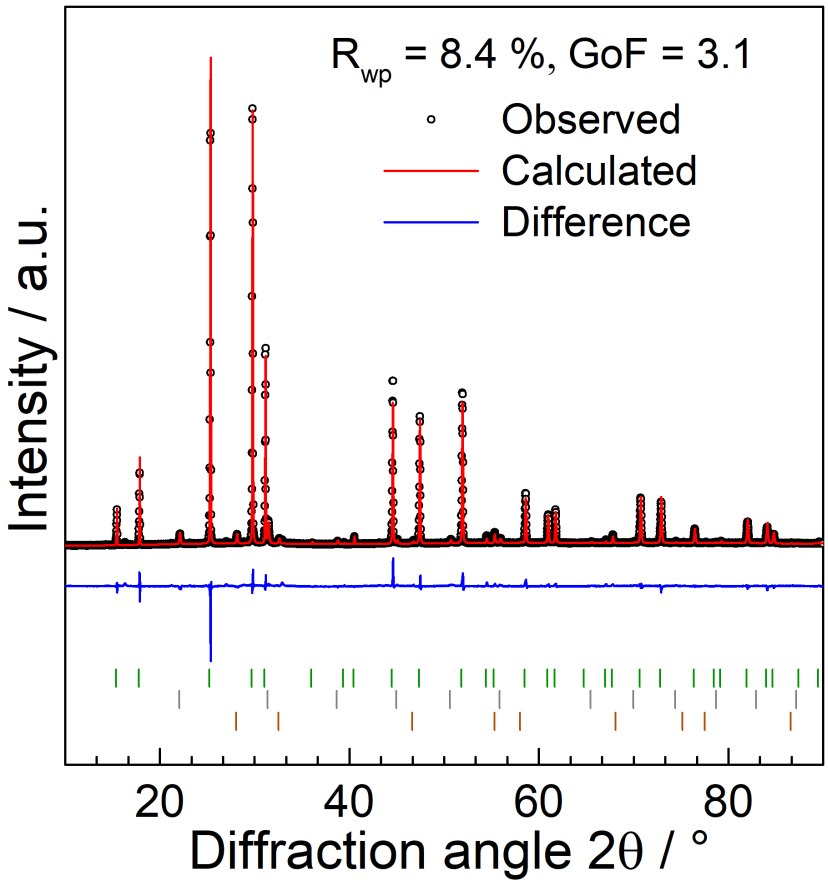

Figure S2: X-ray powder diffraction data for Li_6PS_5Br after 30 min heating followed by quenching and corresponding Rietveld refinement. Experimental data are shown in black and the red line denotes the calculated pattern, while the difference profile is shown in blue. Calculated positions of the Li_6PS_5Br, Li_3OBr and LiBr Bragg reflections are shown as green, gray and dark orange vertical ticks, respectively.

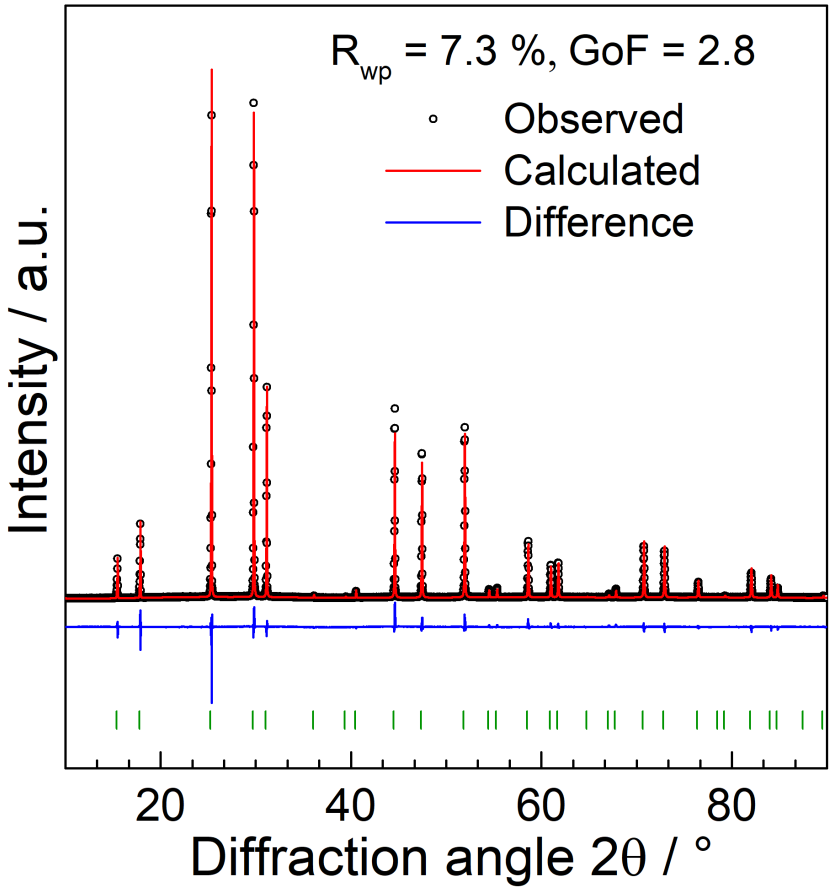

Figure S3: X-ray powder diffraction data for Li_6PS_5Br after 300 min heating followed by quenching and corresponding Rietveld refinement. Experimental data are shown in black and the red line denotes the calculated pattern, while the difference profile is shown in blue. Calculated positions of the Li_6PS_5Br Bragg reflections are shown as green vertical ticks, respectively.

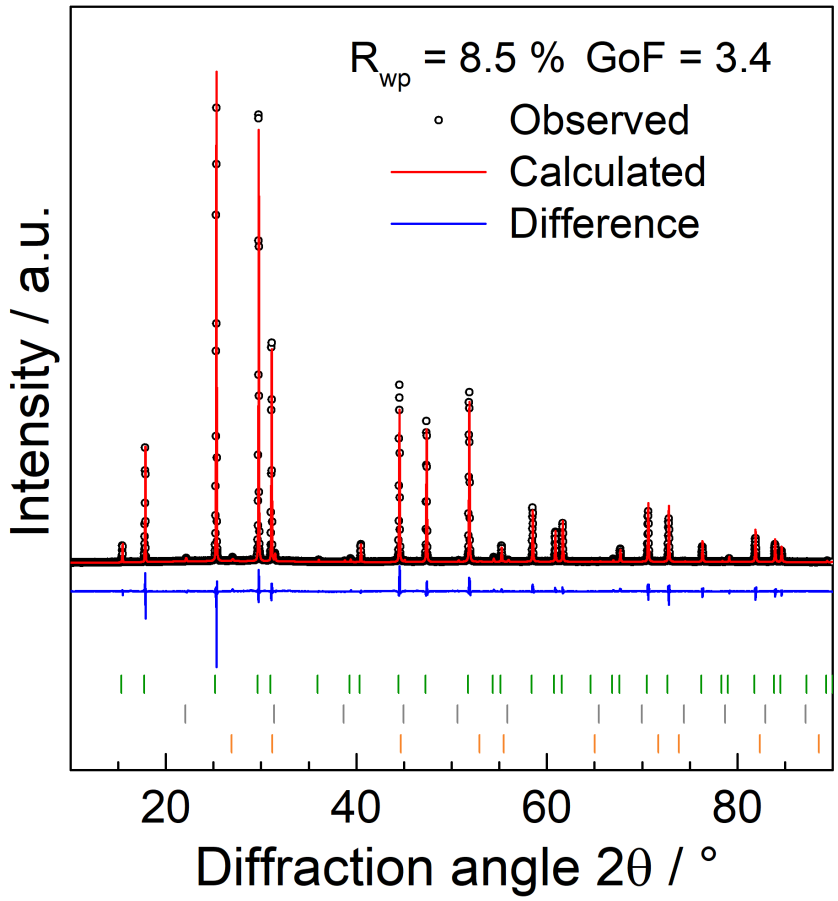

Figure S4: X-ray powder diffraction data for Li_6PS_5Br after 5 min heating followed by standard cooling and corresponding Rietveld refinement. Experimental data are shown in black and the red line denotes the calculated pattern, while the difference profile is shown in blue. Calculated positions of the Li_6PS_5Br, Li_2S and Li_3OBr Bragg reflections are shown as green, gray and orange vertical ticks, respectively.

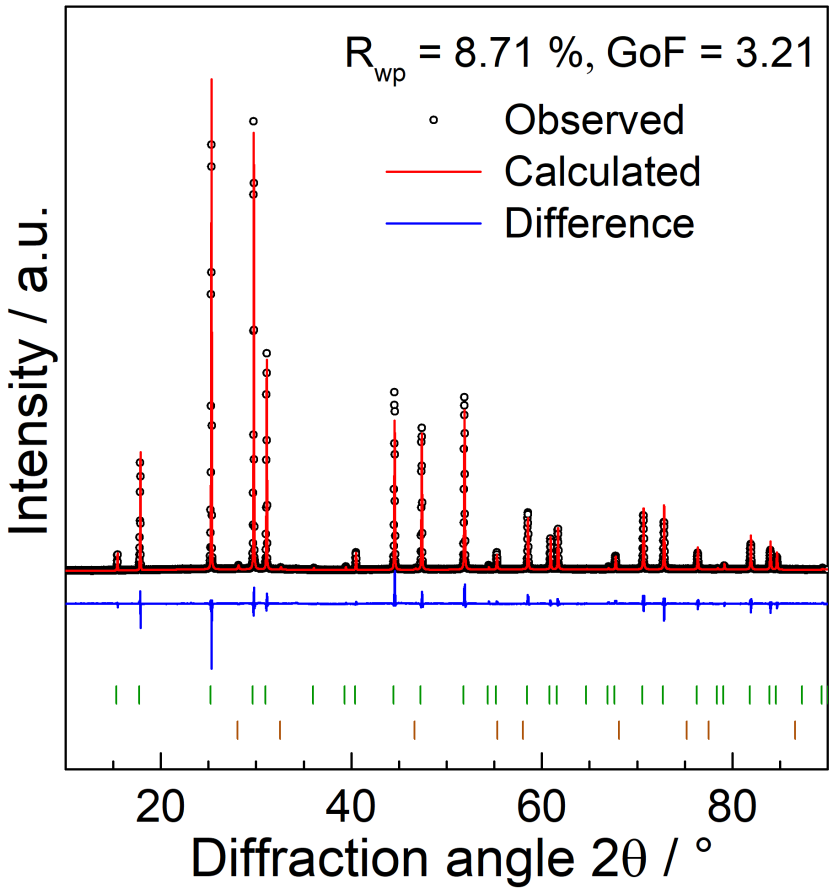

Figure S5: X-ray powder diffraction data for Li_6PS_5Br after 30 min heating followed by standard cooling and corresponding Rietveld refinement. Experimental data are shown in black and the red line denotes the calculated pattern, while the difference profile is shown in blue. Calculated positions of the Li_6PS_5Br and LiBr Bragg reflections are shown as green and dark orange vertical ticks, respectively.

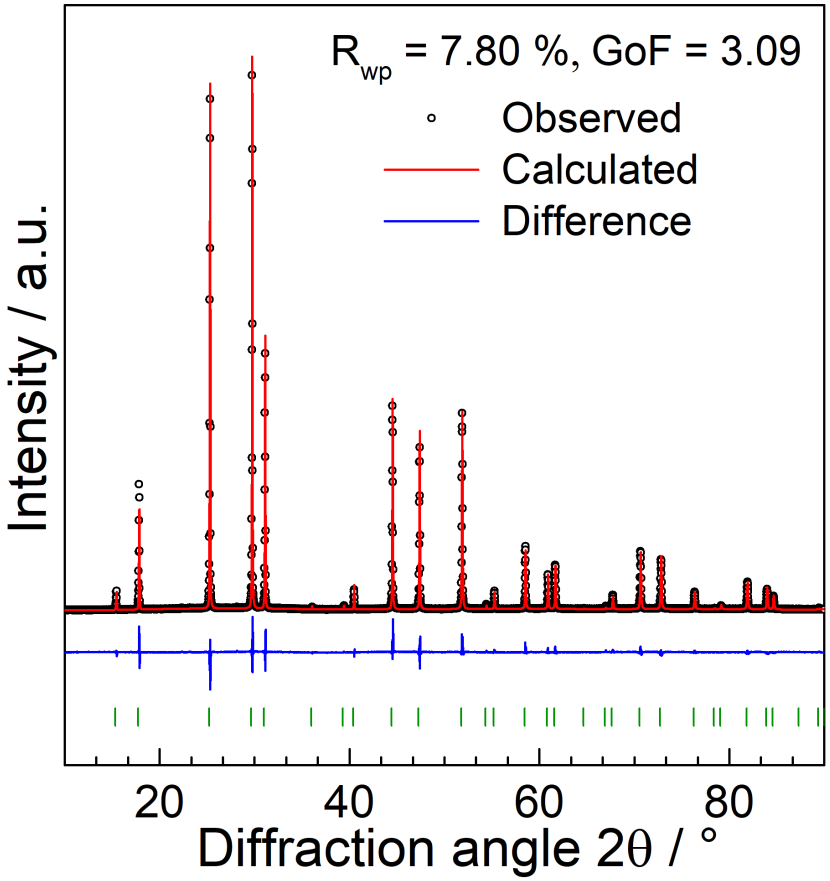

Figure S6: X-ray powder diffraction data for Li_6PS_5Br after 300 min heating followed by standard cooling and corresponding Rietveld refinement. Experimental data are shown in black and the red line denotes the calculated pattern, while the difference profile is shown in blue. Calculated positions of the Li_6PS_5Br Bragg reflections are shown as green vertical ticks, respectively.

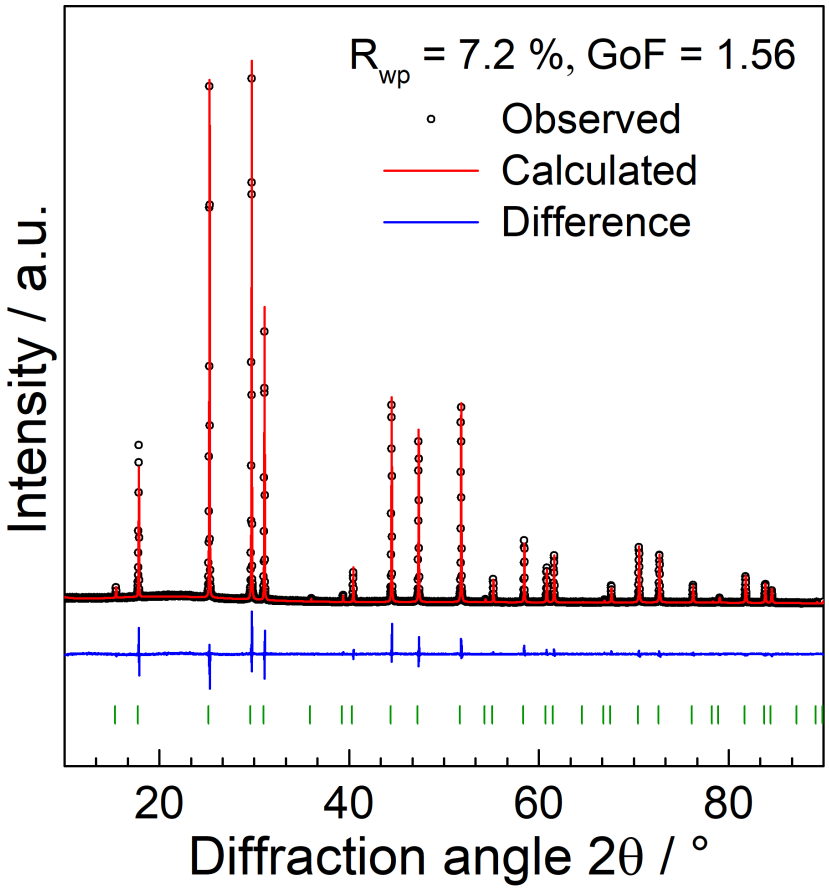

Figure S7: X-ray powder diffraction data for Li_6PS_5Br after 30 min reaction at 550 °C then 5-day cooling and corresponding Rietveld refinement. Experimental data are shown in black and the red line denotes the calculated pattern, while the difference profile is shown in blue. Calculated positions of the Li_6PS_5Br and LiBr Bragg reflections are shown as green and dark orange vertical ticks, respectively.

Table S1. Crystallographic data of after 1 min of heating followed by quenching Li_6PS_5Br from X-ray diffraction. Refined parameters are shown with uncertainty in brackets.

a = 9.96696(3) Å; 0.73 % LiBr R_{wp} = 6.11 % ; GoF = 2.47						
Atom	Wyckoff Site	*x/a*	y/*b*	z/*c*	Occ	B_{eq}/ Å^2
Li1	48*h*	0.3071	0.0251	0.6929	0.4407	3
Li2	24*g*	0.25	0.017	0.75	0.1186	3
Br1	4*a*	1.0	1.0	1.0	0.635(2)	1.25(4)
Br2	4*d*	0.75	0.75	0.75	0.364(2)	0.51(4)
P1	4*b*	1.0	0.5	1.0	1.0	0.93(5)
S1	4*d*	0.75	0.75	0.75	0.635(2)	0.51(4)
S2	16*e*	0.11954(8)	-0.11954(8)	0.61954(8)	1.0	0.93(5)
S3	4*a*	1.0	1.0	1.0	0.364(2)	1.25(4)

Table S2. Crystallographic data after 5 min of heating followed by quenching Li_6PS_5Br from X-ray diffraction. Refined parameters are shown with uncertainty in brackets.

a = 9.96965(3) Å; 0.76 % LiBr R_{wp} = 6.8 % ; GoF = 2.7						
Atom	Wyckoff Site	*x/a*	y/*b*	z/*c*	Occ	B_{eq}/ Å^2
Li1	48*h*	0.3071	0.0251	0.6929	0.4407	3
Li2	24*g*	0.25	0.017	0.75	0.1186	3
Br1	4*a*	1.0	1.0	1.0	0.663(2)	0.91(5)
Br2	4*d*	0.75	0.75	0.75	0.337(2)	0.21(4)
P1	4*b*	1.0	0.5	1.0	1.0	0.50(4)
S1	4*d*	0.75	0.75	0.75	0.663(2)	0.21(4)
S2	16*e*	0.11974(8)	-0.11974(8)	0.61974(8)	1.0	0.50(4)
S3	4*a*	1.0	1.0	1.0	0.337(2)	0.91(5)

Table S3. Crystallographic data after 30 min of heating followed by quenching Li_6PS_5Br from X-ray diffraction. Refined parameters are shown with uncertainty in brackets.

a = 9.97072(5) Å; 1.52 % LiBr; 4.17 % Li_3OBr R_{wp} = 8.4 % ; GoF = 3.1						
Atom	Wyckoff Site	*x/a*	y/*b*	z/*c*	Occ	B_{eq}/ Å^2
Li1	48*h*	0.3071	0.0251	0.6929	0.4407	3
Li2	24*g*	0.25	0.017	0.75	0.1186	3
Br1	4*a*	1.0	1.0	1.0	0.641(3)	0.62(6)
Br2	4*d*	0.75	0.75	0.75	0.358(3)	0.14(5)
P1	4*b*	1.0	0.5	1.0	1.0	0.06(3)
S1	4*d*	0.75	0.75	0.75	0.641(3)	0.14(5)
S2	16*e*	0.1193(1)	-0.1193(1)	0.6193(1)	1.0	0.06(3)
S3	4*a*	1.0	1.0	1.0	0.358(3)	0.62(6)

Table S4. Crystallographic data after 300 min of heating followed by quenching Li_6PS_5Br from X-ray diffraction. Refined parameters are shown with uncertainty in brackets.

a = 9.96866(3) Å; R_{wp} = 7.3 % ; GoF = 2.8						
Atom	Wyckoff Site	*x/a*	y/*b*	z/*c*	Occ	B_{eq}/ Å^2
Li1	48*h*	0.3071	0.0251	0.6929	0.4407	3
Li2	24*g*	0.25	0.017	0.75	0.1186	3
Br1	4*a*	1.0	1.0	1.0	0.624(2)	0.99(5)
Br2	4*d*	0.75	0.75	0.75	0.375(2)	0.29(5)
P1	4*b*	1.0	0.5	1.0	1.0	0.76(3)
S1	4*d*	0.75	0.75	0.75	0.624(2)	0.29(5)
S2	16*e*	0.11976(8)	-0.11976(8)	0.61976(8)	1.0	0.76(3)
S3	4*a*	1.0	1.0	1.0	0.375(2)	0.99(5)

Table S5. Crystallographic data after 1 min of heating followed by standard cooling Li_6PS_5Br from X-ray diffraction. Refined parameters are shown with uncertainty in brackets.

a = 9.98112(3) Å; 0.67 % LiBr R_{wp} = 8.67 % ; GoF = 3.22						
Atom	Wyckoff Site	*x/a*	y/*b*	z/*c*	Occ	B_{eq}/ Å^2
Li1	48*h*	0.3071	0.0251	0.6929	0.4407	3
Li2	24*g*	0.25	0.017	0.75	0.1186	3
Br1	4*a*	1.0	1.0	1.0	0.771(3)	0.75(5)
Br2	4*d*	0.75	0.75	0.75	0.228(3)	0.32(6)
P1	4*b*	1.0	0.5	1.0	1.0	0.22(3)
S1	4*d*	0.75	0.75	0.75	0.771(3)	0.32(6)
S2	16*e*	0.11953(9)	-0.11953(9)	0.61953(9)	1.0	0.22(3)
S3	4*a*	1.0	1.0	1.0	0.228(3)	0.75(5)

Table S6. Crystallographic data after 5 min of heating followed by standard cooling Li_6PS_5Br from X-ray diffraction. Refined parameters are shown with uncertainty in brackets.

a = 9.98577(3) Å; 1.35 % Li_2S; 1.05 % Li_3OBr; R_{wp} = 8.5 % ; GoF = 3.4						
Atom	Wyckoff Site	*x/a*	y/*b*	z/*c*	Occ	B_{eq}/ Å^2
Li1	48*h*	0.3071	0.0251	0.6929	0.4407	3
Li2	24*g*	0.25	0.017	0.75	0.1186	3
Br1	4*a*	1.0	1.0	1.0	0.779(2)	1.19(5)
Br2	4*d*	0.75	0.75	0.75	0.220(2)	0.76(6)
P1	4*b*	1.0	0.5	1.0	1.0	0.55(3)
S1	4*d*	0.75	0.75	0.75	0.779(2)	0.76(6)
S2	16*e*	0.11955(9)	-0.11955(9)	0.61955(9)	1.0	0.55(3)
S3	4*a*	1.0	1.0	1.0	0.220(2)	1.19(5)

Table S7. Crystallographic data after 30 min of heating followed by standard cooling Li_6PS_5Br from X-ray diffraction. Refined parameters are shown with uncertainty in brackets.

a = 9.98162(4) Å; 0.73 % LiBr R_{wp} = 8.7 % ; GoF = 3.21						
Atom	Wyckoff Site	*x/a*	y/*b*	z/*c*	Occ	B_{eq}/ Å^2
Li1	48*h*	0.3071	0.0251	0.6929	0.4407	3
Li2	24*g*	0.25	0.017	0.75	0.1186	3
Br1	4*a*	1.0	1.0	1.0	0.777(3)	0.63(5)
Br2	4*d*	0.75	0.75	0.75	0.222(3)	0.23(7)
P1	4*b*	1.0	0.5	1.0	1.0	0.45(4)
S1	4*d*	0.75	0.75	0.75	0.777(3)	0.23(7)
S2	16*e*	0.1195(1)	-0.1195(1)	0.6195(1)	1.0	0.45(4)
S3	4*a*	1.0	1.0	1.0	0.222(3)	0.63(5)

Table S8. Crystallographic data after 300 min of heating followed by standard cooling Li_6PS_5Br from X-ray diffraction. Refined parameters are shown with uncertainty in brackets.

a = 9.98174(4) Å; R_{wp} = 7.8 % ; GoF = 3.1						
Atom	Wyckoff Site	*x/a*	y/*b*	z/*c*	Occ	B_{eq}/ Å^2
Li1	48*h*	0.3071	0.0251	0.6929	0.4407	3
Li2	24*g*	0.25	0.017	0.75	0.1186	3
Br1	4*a*	1.0	1.0	1.0	0.768(3)	0.84(4)
Br2	4*d*	0.75	0.75	0.75	0.231(3)	0.48(6)
P1	4*b*	1.0	0.5	1.0	1.0	0.38(3)
S1	4*d*	0.75	0.75	0.75	0.768(3)	0.48(6)
S2	16*e*	0.11929(9)	-0.11929(9)	0.61929(9)	1.0	0.38(3)
S3	4*a*	1.0	1.0	1.0	0.231(3)	0.84(4)

Table S9. Crystallographic data after 5-day cooling Li_6PS_5Br from X-ray diffraction. Refined parameters are shown with uncertainty in brackets.

a = 9.99502(4) Å; R_{wp} = 7.2 % ; GoF = 1.56						
Atom	Wyckoff Site	*x/a*	y/*b*	z/*c*	Occ	B_{eq}/ Å^2
Li1	48*h*	0.3071	0.0251	0.6929	0.4407	3
Li2	24*g*	0.25	0.017	0.75	0.1186	3
Br1	4*a*	1.0	1.0	1.0	0.866(3)	1.37(5)
Br2	4*d*	0.75	0.75	0.75	0.133(3)	1.07(7)
P1	4*b*	1.0	0.5	1.0	1.0	0.85(4)
S1	4*d*	0.75	0.75	0.75	0.866(3)	1.07(7)
S2	16*e*	0.11929(9)	-0.11929(9)	0.61929(9)	1.0	0.85(4)
S3	4*a*	1.0	1.0	1.0	0.133(3)	1.37(5)

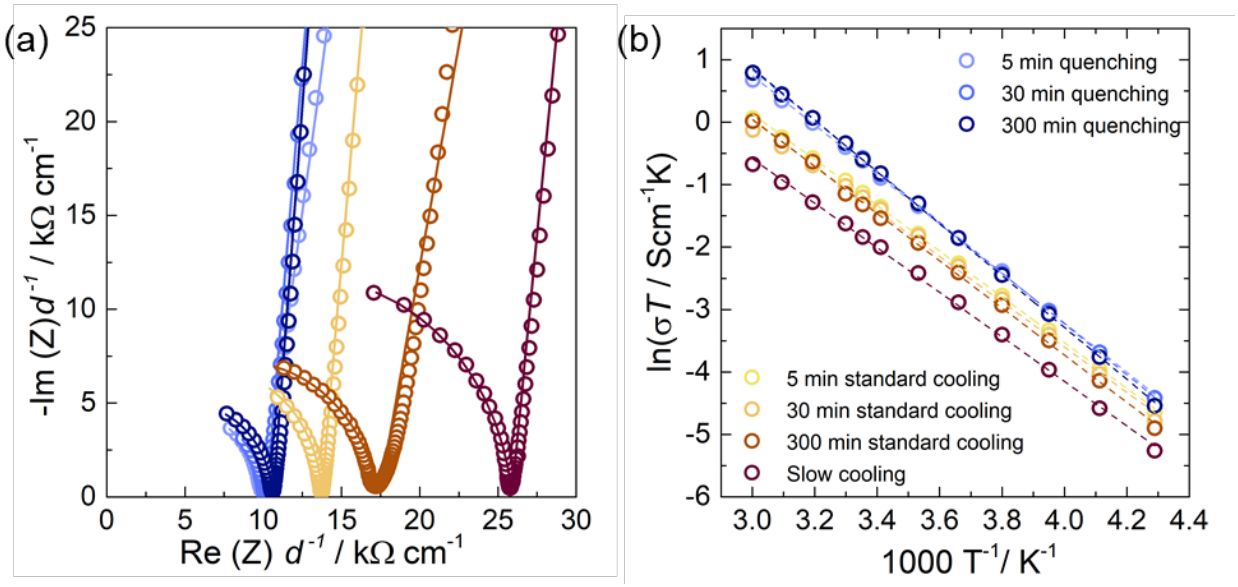

Figure S8: (a) A visual comparison of impedance spectra after using the quenching, standard cooling and slow cooling approach, measured at 253 K. (b) Representative Arrhenius fits of the quenching, standard cooling and slow cooling obtained from impedance spectroscopy.

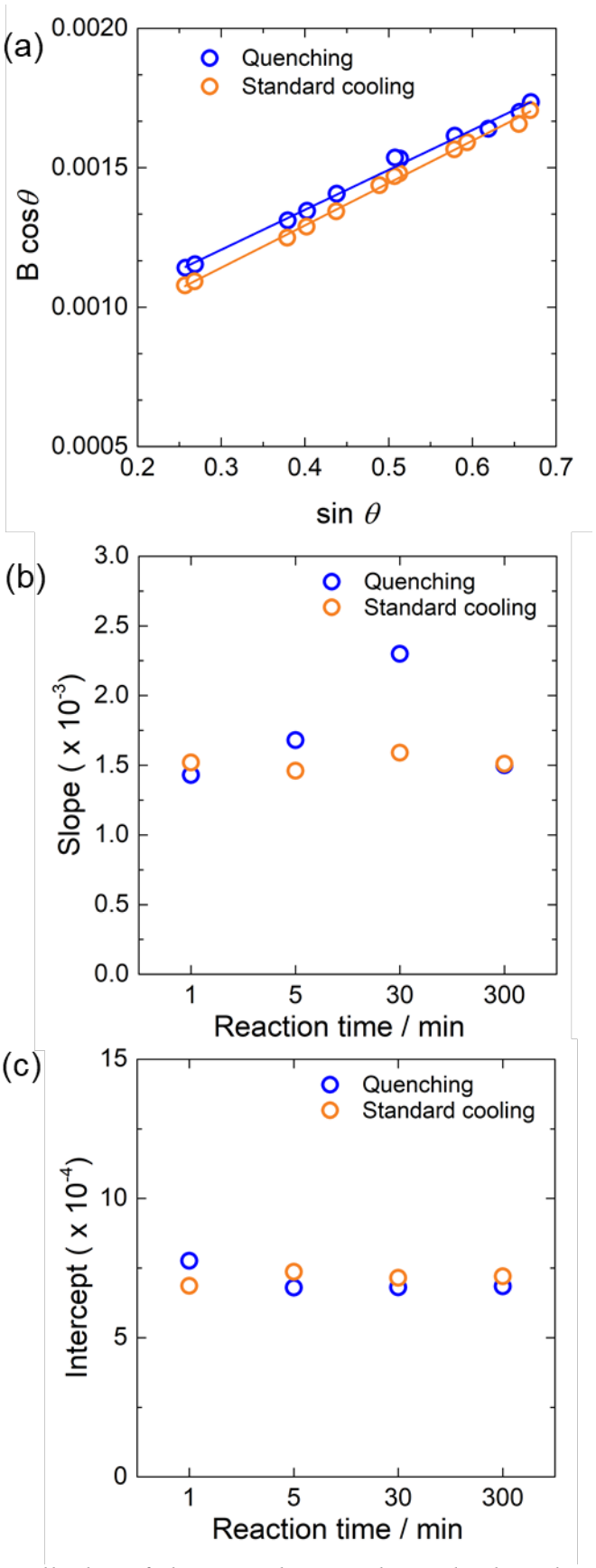

Figure S9: Williamson-Hall plot of the quenching and standard cooling obtained from X-ray diffraction.

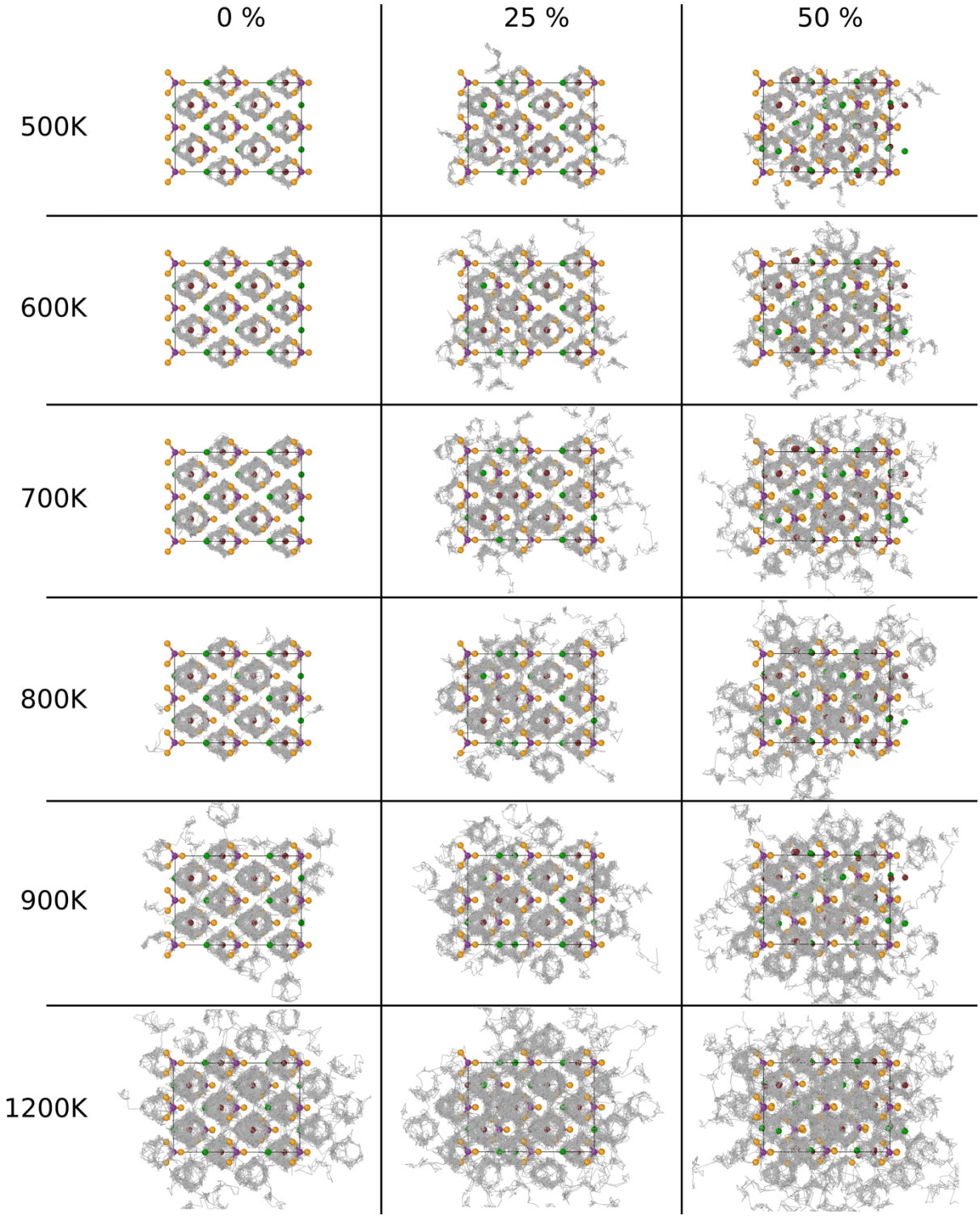

Figure S10: Ab-initio molecular dynamics calculated Li^+ trajectories of Li_6PS_5Br at 0 %, 25 % and 50 % disorder between the S and Br positions after 35 ps of simulation time. Clearly, long-range connecting jumps between the Li clusters occur at much lower temperatures for the disordered structure, compared to the fully ordered cell.

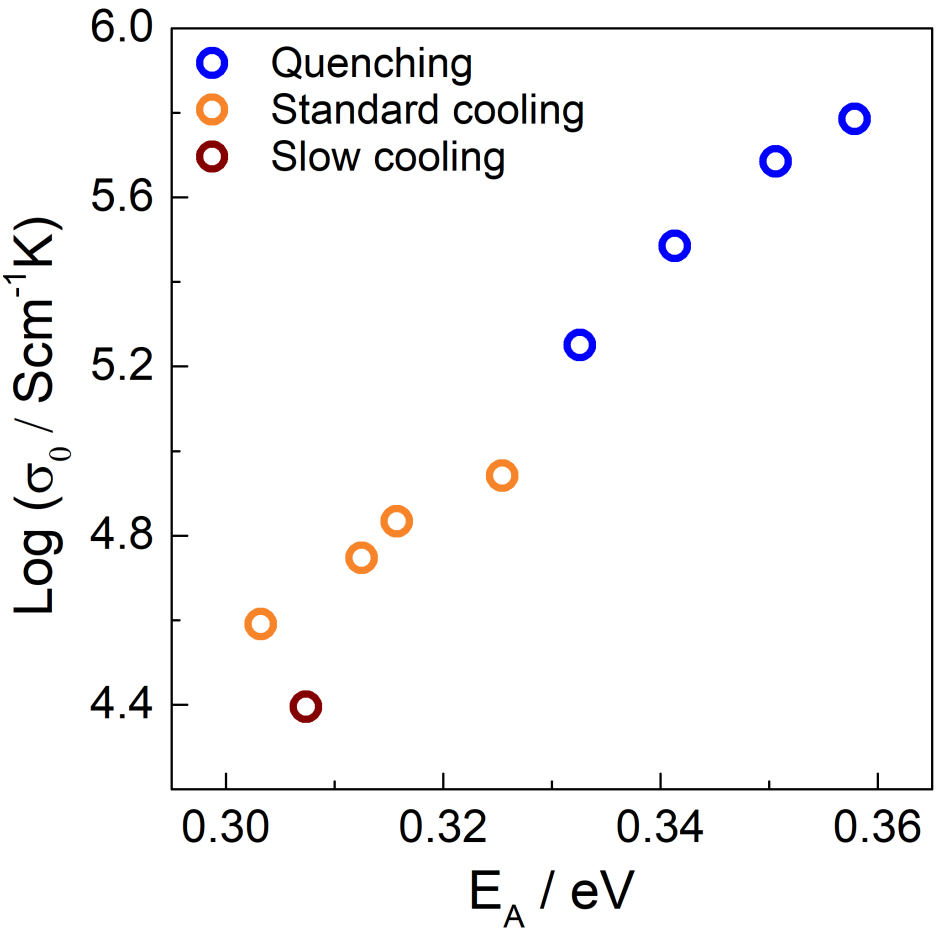

Figure S11: Meyer-Neldel plot of log(σ_0) vs. E_A, showing the enthalpy-entropy compensation of the prefactor with the activation barrier.